

# Intercomparison of Stratospheric Chemistry Models

## under Polar Vortex Conditions

M. Krämer<sup>3</sup>, Ri. Müller<sup>1</sup>, H. Bovensmann<sup>1</sup>, J. Burrows<sup>1</sup>, J. Brinkmann<sup>2,3</sup>, E.P. Röth<sup>2,3</sup>,  
J.-U. Grooß<sup>3</sup>, Ro. Müller<sup>3</sup>, Th. Woyke<sup>3,†</sup>, R. Ruhnke<sup>4</sup>, G. Günther<sup>5,3</sup>, J. Hendricks<sup>5,⊕</sup>,  
E. Lippert<sup>5,⊖</sup>, K. S. Carslaw<sup>6,‡</sup>, Th. Peter<sup>6,⊗</sup>, A. Zieger<sup>6</sup>, Ch. Brühl<sup>6</sup>, B. Steil<sup>6</sup>, R. Lehmann<sup>7</sup>  
and D. S. McKenna<sup>3,§</sup>

<sup>1</sup> Universität Bremen, Inst. für Umweltphysik, 28334 Bremen, Germany

<sup>2</sup> Universität Essen, Inst. für Physikalische Chemie, 45117 Essen, Germany

<sup>3</sup> Forschungszentrum Jülich, Inst. für Stratosphärische Chemie (ICG-1), 52425 Jülich, Germany

<sup>4</sup> Forschungszentrum Karlsruhe, Inst. für Meteorologie und Klimaforschung, 76021 Karlsruhe, Germany

<sup>5</sup> Universität zu Köln, Inst. für Geophysik und Meteorologie, 50931 Köln, Germany

<sup>6</sup> Max-Planck-Institut für Chemie Mainz, Abt. Chemie der Atmosphäre, 55020 Mainz, Germany

<sup>7</sup> Alfred-Wegener-Institut für Polar- und Meeresforschung Potsdam 14473 Potsdam, Germany

---

<sup>†</sup> now ETAS, 70469 Stuttgart, Germany

<sup>⊕</sup> now DLR Oberpfaffenhofen, Inst. für Physik der Atmosphäre, 82234 Weßling, Germany

<sup>⊖</sup> now Dresdner Bank AG, Frankfurt am Main, Germany

<sup>‡</sup> now University of Leeds, Environment Centre, Leeds, LS2 9JT, UK

<sup>⊗</sup> now Eidgen. Techn. Hochschule Zürich, Inst. für Atmosphärenphysik, 8093 Zürich, Switzerland

<sup>§</sup> now NCAR, Atmospheric Chemistry Division, Boulder, CO 80307-3000, USA

Submitted to: Journal of Atmospheric Chemistry

## Abstract

Several stratospheric chemistry modules from box, 2-D or 3-D models, have been intercompared. The intercomparison was focused on the ozone loss and associated reactive species under the conditions found in the cold, wintertime Arctic and Antarctic vortices. Comparisons of both gas phase and heterogeneous chemistry modules show excellent agreement between the models under constrained conditions for photolysis and the microphysics of polar stratospheric clouds. While the mean integral ozone loss ranges from 4 – 80% for different 30 – 50 days long air parcel trajectories, the mean scatter of model results around these values is only about  $\pm 1.5\%$ . In a case study, where the models employed their standard photolysis and microphysical schemes, the variation around the mean percentage ozone loss increases to about  $\pm 7\%$ . This increased scatter of model results is mainly due to the different treatment of the PSC microphysics and heterogeneous chemistry in the models, whereby the most unrealistic assumptions about PSC processes consequently lead to the least representative ozone chemistry. Furthermore, for this case study the model results for the ozone mixing ratios at different altitudes were compared with a measured ozone profile to investigate the extent to which models reproduce the stratospheric ozone losses. It was found that mainly in the height range of strong ozone depletion all models underestimate the ozone loss by about a factor of two. This finding corroborates earlier studies and implies a general deficiency in our understanding of the stratospheric ozone loss chemistry rather than a specific problem related to a particular model simulation.

# 1 Introduction

Since the early 1970s numerical simulations of stratospheric chemistry have been used to further our understanding of the stratosphere, because the important role of particularly the ozone chemistry in these altitudes has become more and more obvious. A detailed understanding and an accurate numerical description of the stratospheric chemical situation is the basis for a reliable numerical prediction of its future development as a function of human activities. Consequently, it should be expected that, even if the stratospheric chemical schemes and the numerical methods and assumptions may vary from model to model (although all models seek to describe the same chemical and physical processes), the results of chemistry simulations for the same stratospheric conditions are similar. The results of simulations should agree even more closely if the models use identical input parameters for chemical rate constants and photolysis frequencies. An additional expectance to the models is that the results of the simulations should be in agreement with measurements. However, for some time it has been known that many chemical simulations underestimate the magnitude of polar ozone loss (e.g. Hansen et al., 1997; Becker et al., 1998; Woyke et al., 1999; Becker et al., 2000a) deduced from various observations (Müller et al., 1996; Rex et al., 1998; Goutail et al., 1999).

An extensive comparison of global stratospheric chemistry 2D and 3D models has been conducted by Park et al. (1999). In contrast, we compare in this study the chemistry modules of different stratospheric models under defined conditions along different air mass trajectories. We present an intercomparison of eight distinct chemical schemes used by participants in the German ‘Ozonforschungsprogramm’ (Ozone Research Program 1990 – 2000; for a description of the models see Section 2.1). To ensure the relevance of the intercomparison, it focuses on ozone loss and the major chemical species related to the chemical destruction of ozone under Arctic and Antarctic stratospheric winter conditions. Moreover, some of the results of the model simulations are compared with measurements. Thus, the consistency of the model results was tested under relevant requirements.

Two sets of intercomparison studies were conducted (an overview of the different scenarios is given in Section 2.3). Firstly, a set of intercomparisons were performed with the same photolysis rates, microphysics of Polar Stratospheric Clouds (PSC) and HCl source chemistry (*prescribed runs*, for detail see Section 3.1). This set of studies serves primarily to estimate the general agreement of the different stratospheric chemical models under prescribed boundary conditions. Additionally, the following subset of studies was performed: the gas phase chemistry modules of the various models are compared, the impact of the use of individual photolysis modules

on model simulations is discussed, the heterogeneous chemistry modules are compared and the influence of the heterogeneous chemistry on model results is shown. The results of the prescribed studies are presented in Section 3.3.

Secondly, model simulations were conducted in which each model used its standard photolysis and microphysics scheme and HCl source chemistry (*unprescribed runs*, for detail see Section 4.1). With the unprescribed studies, the actual differences between the models and, moreover, their agreement with measurements is investigated by comparing model results with measured profiles of several chemical species. The results of the unprescribed studies are presented in Sections 4.2 and 4.3.

## 2 Overview of the intercomparison studies

### 2.1 Participating models

The institutions participating in the model intercomparison are listed in Table 1 and the various box, 2-D and 3-D stratospheric chemistry models are briefly described in Table 2. A citation is given for the photolysis, gas phase and heterogeneous chemistry code employed by each model. The model acronyms are printed in the colours to be used when representing the results of the respective model. All models were operated in a box mode for the intercomparison. The time development of temperature, pressure and solar zenith angle was prescribed along actual air mass trajectories. The timestep of the data input as well as the output timestep was one hour. All models used rate constants compiled by DeMore et al. (1997).

### 2.2 Species compared

The species to be compared in the model intercomparison are divided into two groups: The first group contains  $\text{O}_3$ ,  $\text{HNO}_3$ ,  $\text{ClOX}$  ( $=\text{ClO} + 2\text{Cl}_2\text{O}_2$ ),  $\text{ClONO}_2$ ,  $\text{HCl}$  and the particle surfaces  $\text{S}_{\text{STS,NAT,ice}}$ . This group is discussed in Section 3.3 for several selected scenarios. The second group, containing  $\text{N}_2\text{O}_5$ ,  $\text{BrO}$ ,  $\text{NO}$ ,  $\text{NO}_2$ ,  $\text{OH}$  and  $\text{HO}_2$ , is presented on a model intercomparison website (see Appendix), where a comprehensive collection of the initial data and simulation results for all participating models is available.

### 2.3 Description of the scenarios

For the intercomparison of the various models a set of scenarios was compiled that allows different modules of the models to be compared and reflects the meteorological and chemical

conditions in the Arctic and Antarctic winter stratosphere. An overview of the scenarios is shown in Tables 3 and 4, the associated trajectory temperatures and Solar Zenith Angles (SZA) are shown in Figure 1. Two groups of scenarios are considered in the model intercomparison which are described in the following.

### 2.3.1 Prescribed Arctic and Antarctic scenarios

In the prescribed scenarios, the photolysis frequencies and the microphysics of PSC are standardized to ensure that only the actual chemistry module may cause differences in the results. The chemical reactions embedded in each module have not been prescribed with the exception of the HCl source reactions (for details of the prescriptions see Section 3.1).

The Arctic and Antarctic winters of the year 1995 were chosen for the prescribed model intercomparison studies. The intercomparisons start with the end of the polar nights (Arctic: 11 Jan., Antarctic: 30 July, see Figure 1 and Tables 3 and 4) and extend towards the end of the lifetime of the polar vortices (Arctic: 31 March, Antarctic: 31 Oct.). This time period is covered by two trajectories based on meteorological fields (denoted as trajectories 1 and 2) on the 475K level whereas the second trajectory is initialized at the endpoint of the first. The description of chlorine activation is tested in the first scenarios represented by trajectories 1, while the second scenarios (trajectories 2) serve to investigate chlorine deactivation processes. Both the Arctic and Antarctic trajectories remain inside the respective vortex<sup>1</sup>. The trajectories are calculated from the meteorological database of UKMO (United Kingdom Meteorological Office).

In the *Arctic scenarios* ARCTIC 1 and 2 the temperature falls below the PSC - formation point at the beginning of trajectory 1 (see Figure 1) and again several times with progressing trajectory time, finally shortly before the vortex breaks up (trajectory 2). In order to compare the gas phase modules of the models, two model runs along both Arctic trajectories are performed. Firstly, model runs including only gas phase chemistry are conducted (ARCTIC 1 (GPH) and ARCTIC 2 (GPH), see Tables 3 and 4). In these model runs the complete activation of chlorine and bromine is included in the initialization (for more detail see Section 3.2 on gas phase initialization). This allows the study of the gas phase ozone loss cycles and the reformation of halogen reservoir species. An additional model run is performed for ARCTIC 1 (GPH), where each model uses its individual photolysis frequencies, showing the influence of the individual

---

<sup>1</sup>For the Arctic scenarios 420 and 600K levels are additionally evaluated; they are not shown in Figure 1, but are available on the model intercomparison website, see Appendix.

representation of photolysis on the time evolution of the chemical species when compared with the run with standardized photolysis frequencies.

Secondly, model runs including the heterogeneous chemistry modules are performed (ARCTIC 1 (GPH + HET) and ARCTIC 2 (GPH + HET)). This allows conclusions to be drawn on the impact of heterogeneous chemistry on the various chemical species and, because of the different ways heterogeneous chemistry is implemented in each model, to compare the heterogeneous chemistry modules of the models.

In the *Antarctic scenarios* ANTARCTIC 1 and 2, trajectory 1 (Figure 1) starts with temperatures below the ice-frost point; the temperature increases steadily in the course of trajectories 1 and 2. In the model runs along both Antarctic trajectories the modules for gas phase and heterogeneous chemistry are active (ANTARCTIC 1 (GPH + HET) and ANTARCTIC 2 (GPH + HET)).

### 2.3.2 Unprescribed Arctic scenarios

In the unprescribed scenarios each model is operated individually, on the one hand to examine the extent to which each model can reproduce the ozone loss and the associated species described in section 2.2, and on the other hand to evaluate the actual difference between the models.

Therefore, model calculations are compared with measurements in the Arctic winter 1995. This study is adopted from Woyke et al. (1999), who used the FACSIMILE model (FZ-Jülich-version, see Table 1). The time period of this ARCTIC CASE STUDY ranges from early winter 1994 until early spring 1995 (see Tables 3 and 4), during which measurements of vertical profiles of several chemical species are available. Six 50 day backward trajectories on different levels cover this period. A detailed description of this study is given in Section 4.1.

Here the study is repeated for all models participating in the model intercomparison. The model calculations are performed using individual heterogeneous chemistry settings, photolysis frequencies and HCl source reactions, i. e. they present the largest possible scatter of model results. To study the model scatter, the trajectory at the 475K – level was taken (see Figure 1, lower left and right panels). It can be seen that the temperature was relatively high on average and it was quite dark along the trajectory, but nevertheless PSC formation occurs several times. To test the agreement of models with measurements, simulation results at the end of the six trajectories are compared with the measured profiles.

### 3 Prescribed Arctic and Antarctic scenarios

#### 3.1 Prescriptions

##### 3.1.1 Standardized photolysis frequencies

The standardized photolysis frequencies are calculated using the formula derived by R oth (1992) (see also Table 3):

$$j = a \cdot \exp \left( b \cdot \left( 1 - \frac{1}{\cos(c \cdot \chi)} \right) \right) \quad (1)$$

where  $j$  is the photolysis frequency and  $\chi$  is the SZA. The values of the parameters  $a$ ,  $b$  and  $c$  are tabulated for each scenario for 115 photolysis reactions at the mean latitude, albedo and O<sub>3</sub> and O<sub>2</sub> columns of the respective trajectory.

The impact of photolysis on the mixing ratios of the chemical components also depends on the maximum SZA allowed in the model calculations. For example, it is estimated by the model MPIC for the ARCTIC CASE STUDY (475K) that the total percentage ozone loss is 25% if the maximum SZA is 90  and increases to 31% when the maximum SZA is raised to 92 ; this is the case since the photolysis of Cl<sub>2</sub> and Cl<sub>2</sub>O<sub>2</sub> already proceeds in twilight and determines the time span available for ozone destruction (i.e. Becker et al., 2000b and Rex et al., 2000). Therefore, for the model intercomparison

$$j = 0 \quad \text{for} \quad \chi > 100^\circ \quad \text{or} \quad (c \cdot \chi) > 90^\circ \quad (2)$$

is defined as the upper truncation condition for the calculation of the photolysis rates.

##### 3.1.2 Standardized PSC microphysics

Since the modules for heterogeneous chemistry reactions are to be compared here, the potential influence of different PSC microphysics on heterogeneous chemistry is suppressed by using standardized PSC microphysics described in the following.

The background supercooled liquid ternary solution (STS) aerosol particles are formed from gas phase H<sub>2</sub>SO<sub>4</sub> and H<sub>2</sub>O. Owing to its very low vapor pressure, all H<sub>2</sub>SO<sub>4</sub> is assumed to be in the condensed phase. HNO<sub>3</sub> equilibrates between the gas and particle phase according to the actual thermodynamic conditions. The resulting particle number density distribution  $N(r)$  is assumed to be lognormal with a given width  $\sigma$ .

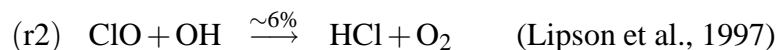
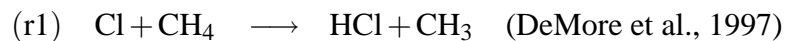
Therefore, the total STS particle surface density ( $S_{\text{STS}}$ ) at the starting point of each respective trajectory depends on the prescribed mixing ratio of H<sub>2</sub>O, H<sub>2</sub>SO<sub>4</sub> and HNO<sub>3</sub>, the prescribed number of STS particles ( $N_{\text{STS}}$ ) as well as on the initial pressure and temperature. NAT (nitric

acid trihydrate) and ice particles nucleate when a prescribed supersaturation is reached. Then, a defined number of particles  $N_{\text{NAT}}$  or  $N_{\text{ice}}$  appear. Note that in the case of NAT formation, STS and NAT particles coexist, whereby the number of STS particles is reduced by the number of NAT particles. In the case of ice formation, STS, NAT and ice particles coexist. The standardized values for PSC microphysics ( $N_{\text{STS}}$ ,  $N_{\text{NAT}}$ ,  $N_{\text{ice}}$ ,  $\text{Supersat}_{\text{NAT}}$ ,  $\text{Supersat}_{\text{ice}}$ ) and the initialization of the background STS aerosol ( $\text{H}_2\text{SO}_4$ ,  $\sigma$ ,  $S_{\text{STS}}$ ,  $S_{\text{ice}}$ ) are listed in Table 5 for all prescribed scenarios. The respective initial mixing ratios of gas phase  $\text{H}_2\text{O}$  and  $\text{HNO}_3$  are shown in Table 6.

### 3.1.3 Standardized HCl source reactions

A third standardization was introduced retrospectively as a result of the model intercomparison. It was found that the strength of HCl formation varies substantially with the different chemical reaction pathways implemented in the models <sup>2</sup>.

This is demonstrated by means of the ARCTIC 1 (GPH) scenario (Figure 2), where the four most important possible source reactions for HCl are enabled one after another using the KASIMA model. As also shown in Figure 2, the ozone loss (and likewise the other chemical species) is not strongly affected by the strength of HCl source reactions. As a result of this sensitivity study, only the two major source reactions for HCl that are unequivocally supported by laboratory measurements



are enabled in all prescribed scenarios of the model intercomparison.

## 3.2 Initialization of gas phase chemistry

The initial mixing ratios of the gas phase species for the various scenarios are listed in Table 6.

The values for the first scenarios ARCTIC 1 and ANTARCTIC 1, are calculated for the starting points of the respective trajectories using the two – dimensional MPIC model (see Table 3). For the scenario ARCTIC 1 (GPH), where heterogeneous chemistry is not taken into account, these initial conditions were modified (‘activated’) to simulate realistic ozone destruction: all  $\text{HCl} + \text{ClONO}_2$  was transformed into ClO whereas HCl and ClONO<sub>2</sub> were initialized as zero.

---

<sup>2</sup>in their original configuration, the participating models took into account the following HCl production channels (reactions see Figure 2): AWI, BRAPHO, CLaMS, MPIC: r1 and r2; KASIMA: r1, r2, r4; COMMA, EURAD-TS: r1, Mainz-FACSIMILE: r1, r2, r3.



Similarly, the inorganic bromine species were transformed into BrO, and  $\text{N}_2\text{O}_5$  into  $2 \cdot \text{HNO}_3$ . These parameters are listed separately in Table 6 for ARCTIC 1 (GPH) and (GPH + HET), all other initial values are identical for both scenarios.

As initial values for the second scenarios ARCTIC 2 and ANTARCTIC 2, the respective values at the end of the first scenarios (calculated by the BRAPHO or CLaMS model) are taken. Along the trajectory of ANTARCTIC 1 ice particles are formed for a certain time and may fall out by sedimentation. Therefore, the initial values of ANTARCTIC 2 are modified: (a) the initialization is artificially dehydrated by taking the minimum value of  $\text{H}_2\text{O}$  during ANTARCTIC 1; (b) denitrification is taken into account by initializing ANTARCTIC 2 with one quarter of the  $\text{NO}_y$  of ANTARCTIC 1.

### 3.3 Agreement of the models in the prescribed scenarios

A summary of the evaluations for the prescribed scenarios is presented here. We show only the most relevant results for the 475K level, since the findings for 420K and 600K levels are very similar and are reported on the website described in the Appendix.

#### 3.3.1 Scatter of the percentage ozone loss

As a measure of the agreement among the models we chose the scatter of all model results around the mean ozone loss in percent at the end of each scenario (see Table 7). The mean ozone loss covers a wide range from about 4% to 80% depending on the specific scenario. Irrespective of the strength of the ozone loss, the standard deviation of the individual model results from the mean values ranged between only 0.2 – 3.3% (absolute units) for the prescribed scenarios, i.e. very good agreement of the models was achieved under prescribed conditions.

The simulated absolute loss rates reach peak values of 40 – 60 ppb/day for the Arctic scenarios but only for very short periods; because of the lack of sunlight along the trajectories also very low loss rates of  $\approx 5$  ppb/day occur for the Arctic cases, even during the period of strong chlorine activation. For the Antarctic scenarios, peak values of  $\approx 130$  ppb/day for the ozone loss rate are simulated by the participating models. Owing to varying solar insolation, loss rates vary as well; even during the period of strong chlorine activation loss rates below  $\approx 60$  ppb/day occur.

In Figure 3 (bottom three panels), the percentage ozone loss of each model in the course of the prescribed scenarios is shown (the percentage ozone losses at the beginning of the second scenarios are adjusted to the mean ozone loss at the end of the respective first scenarios). Again

it can be seen that the agreement of the models is good in the prescribed scenarios<sup>3</sup>. The spread of the ozone loss rates of the various models is mainly due to different ClO concentrations (see Figure 4). Even for the ARCTIC 1 (GPH + HET) scenario with prescribed photolysis rates (Figure 4, right panel), ClO concentrations simulated for the last 5 days of the scenario with the KASIMA (green) and MPIC (pink) models are considerably greater and those of the COMMA model (olive) considerably smaller than the average. The different ClO concentrations and thus the spread in ozone loss rates is due to the different set-up of the heterogeneous chemistry in the models; for the ARCTIC 1 (GPH) scenario –pure gas phase– a much smaller spread of the ozone loss rates is found (Figure 4, left panel).

### 3.3.2 Model run with individual photolysis schemes

Additional model runs were performed that are identical to the prescribed ARCTIC 1 (GPH) scenario, except that each model uses its individual photolysis module (with the same overhead ozone profile as in the prescribed scenario). Thus, the impact of different photolysis schemes on evolution over time of the chemical species can be investigated. The result, shown in Table 7 (lower line) and in Figure 3 (top left panel), can be compared directly to the original prescribed run shown in the panel below. The influence of different photolysis modules on the development of the ozone loss is not very large for any of the models, the standard deviation of the mean ozone loss only increases from 0.3% to 1%. As in this model run the ozone profile is prescribed, the scatter of model results could increase if individual ozone profiles are used. However, sensitivity runs with the CLaMS model show that this influence is negligible.

Most notable in the model run with individual photolysis schemes is that in comparison to KASIMA (which uses the standard photolysis scheme after R<sup>o</sup>th, 1992; green curve) all models show a slightly smaller ozone loss when their individual photolysis modules are used.

### 3.3.3 Sensitivity of ozone loss to uncertainties in trajectory temperatures

To test the sensitivity of model results to potential errors in the trajectory temperature, two additional model simulations for each scenario were performed using the chemistry scheme from the CLaMS model, each with  $\pm 2\text{K}$  offsets to the trajectory temperature.

It is found that: a) for the scenarios without heterogeneous chemistry, the uncertainty of the percentage ozone loss caused by the temperature is very small (about  $\pm 0.3\%$ ) being in the same

---

<sup>3</sup>However, particularly in the ARCTIC 1 (GPH) and ARCTIC 2 (GPH+HET) scenarios the MPIC (pink) model is not comparable with the other models as explained in Table 2. Therefore, it is not included in the calculation of the mean ozone losses and standard deviations of these scenarios.

range as the scatter of model simulations; b) in the prescribed cases including heterogeneous chemistry, the uncertainty of the ozone loss caused by the temperature variation becomes much more important (up to about 15% for ANTARCTIC 2). This is because the formation of NAT with subsequent ozone destruction can be suppressed/enhanced by higher/lower temperature.

### 3.3.4 Detailed example of model agreement under prescribed conditions

As a detailed example for the good agreement of the models in the prescribed scenarios, all key chemical species (see Table ??) are shown for the ANTARCTIC 2 (GPH + HET) scenario in Figures 5 and 6 (left panels). NAT is formed several times between day -50 and -30. This leads to activation of chlorine from the  $\text{ClONO}_2$  and  $\text{HCl}$  reservoirs with subsequent severe ozone destruction of 2.4ppm (see Table 7). After this time period, the Antarctic vortex begins to weaken (see Figure 1). The reservoirs recover while the chlorine species  $\text{ClO}$  and  $\text{Cl}_2\text{O}_2$  disappear,  $\text{HNO}_3$  decreases and  $\text{O}_3$  stabilizes at a low level. Over the course of this simulated time period, which includes very strong chemical transformation processes, the models show quite a good agreement for all species. This good agreement suggests that the current knowledge of stratospheric gas phase chemistry is well represented in all models.

## 4 Unprescribed Arctic Case Study

### 4.1 Description of the Arctic Case Study

Vertical profiles of ozone, chlorine monoxide, bromine monoxide and  $\text{HCl}$  were recorded in the Arctic vortex in February 1995. Model calculations were performed along six 50-day backward trajectories at six isentropic levels (see Table 3), all ending at the measured profiles. The trajectories start in the early winter of 1994, when the gas phase chemistry is still unperturbed by heterogeneous chemical processing, and end in February 1995 when ozone has already been destroyed. Comparison of the model results at the end of the trajectories with the measured profiles therefore allows an assessment of the performance of the stratospheric chemistry schemes implemented in the models (see Section 4.3).

As mentioned above, the photolysis rates, PSC microphysics and the  $\text{HCl}$  source reactions are chosen individually in each model in the ARCTIC CASE STUDY. Therefore, it is also suitable for investigating the influence of, in particular, different settings of PSC microphysics and heterogeneous chemistry on the model calculations. This is done for the 475K level (see Section 4.3), the respective trajectory is shown in Figure 1 (for the sake of brevity the trajectories

at the other levels are not shown here).

The ARCTIC CASE STUDY is discussed in detail by Woyke et al. (1999). Only a summary of the most important premises is given here.

*Measurements:* The accuracy of the measurement of ClO is 20%, for BrO it is 30%, for  $O_3 < 2\%$  and for HCl 10%. The ozone loss derived from the balloon observations at the 480 – 500K level is confirmed by various other methods: satellites (HALOE, POAM), Match and Lidar.

*Initialization of model runs:* For this study a very careful initialization is necessary, that means a good description of the stratospheric chemical conditions at the beginning of the trajectories. The initial values for the model runs are based on in situ measurements of long-lived tracers: the chemical species of interest are derived from empirical correlation functions between their mixing ratios and those of the measured tracer. Through this procedure, diabatic descent is taken into account in the initialization (data of initialization are reported in Woyke et al., 1999).

*Sensitivity studies:* A variety of sensitivity studies were carried out with FACSIMILE (FZ-Jülich version) to ensure the validity of the model results: for each level an ensemble of 13 different trajectories, all ending around the point of the balloon measurements, was considered. Very similar results were obtained for all trajectories at each level. Furthermore, the temperature, the initial  $HNO_3$  mixing ratio and the aerosol surface area were varied within reasonable limits and denitrification processes are simulated by removing  $HNO_3$  permanently during PSC existence. The results of the sensitivity runs are within the limits given by the use of the trajectory ensembles.

## 4.2 Agreement of the models in the unprescribed Arctic Case Study

As an example of unprescribed model conditions, the mean percentage ozone loss is shown for the ARCTIC CASE STUDY (475K) in Table 7. The scatter of model results around the mean reaches 6.7% (absolute units), which is about twice the maximum value (3.3%) of the prescribed model runs. This larger scatter is most likely not caused by the different photolysis schemes as can be seen from Table 7: the scatter around the mean ozone loss in the ARCTIC 1 (GPH)<sup>ind. photol. rate</sup> scenario is only 1%. This argument can also be applied to the ARCTIC CASE STUDY because the zenith angles of the two scenarios are comparable (see Figure 1).

The settings of PSC microphysics and heterogeneous chemistry are found to be the cause of the larger scatter of the model simulations, where two main sources are identified: the supersaturation  $S_{NAT}$  required for NAT formation and the reaction probability  $\gamma$  of the heterogeneous

reaction on NAT:  $\text{ClONO}_2 + \text{HCl} \rightarrow \text{Cl}_2 + \text{HNO}_3$ . As a function of these settings, three groups of models are found (see Figures 5 and 6 (right panels)):

**Model group 1** ( $S_{\text{NAT}} > 1$ ,  $\gamma = f(1/T) \rightarrow$  most realistic assumptions with  $S_{\text{NAT}} = 10$ ): In the first model group the chlorine activation from the  $\text{ClONO}_2$  and  $\text{HCl}$  reservoirs starts later (day -29) than for group 2 or 3 (day -39). This is because in the first group  $S_{\text{NAT}} > 1$ , i. e. a lower temperature is needed to form NAT than in the case of  $S_{\text{NAT}} = 1$  (at  $T = 195\text{K}$ ). At day -39 the temperature is only slightly below 195K and a lower temperature is not reached until day -29 and again at day -20 (Figure 1, lower left panel).

In addition, the reduction of  $\text{ClONO}_2$  and  $\text{HCl}$  due to the occurrence of PSC is weaker in group 1 than for the other groups. The reason is the temperature dependence of the heterogeneous reaction probabilities  $\gamma = f(1/T)$ , expressing that the strength of the activation of chlorine increases with decreasing temperature. Strong activation only takes place if the temperature remains clearly below  $T_{\text{NAT}}$ , which happens in this scenario at day -20 (see Figure 1).

Both settings of heterogeneous chemistry prevent strong chlorine activation until day -20 and therefore the models in group 1 show the lowest ozone loss.

**Model group 2** ( $S_{\text{NAT}} = 1$ ,  $\gamma = f(1/T)$ ): Because  $S_{\text{NAT}} = 1$ , the chlorine activation already starts at day -39 in group 2, but it is not very pronounced because  $\gamma = f(1/T)$  and  $T$  is only slightly below 195K for a short time. This leads to a stronger ozone loss than for group 1.

**Model group 3** ( $S_{\text{NAT}} = 1$ ,  $\gamma = \text{const}$ ): The models of the third group show the strongest ozone loss, which results in an early (already at day -39 because  $S_{\text{NAT}} = 1$ ) and strong (because  $\gamma = \text{const}$ . does not depend on temperature) chlorine activation.

To summarize, the uncertainties in the knowledge of the heterogeneous processes (composition of particles, PSC formation temperature, heterogeneous reaction rates) in the stratosphere are reflected here by the scatter of model results. As a result of the model intercomparison we conclude that if the assumptions about heterogeneous processes on PSCs are not realistic the simulations of stratospheric ozone chemistry will not be representative. Therefore, an improvement of the understanding of the microphysics and chemistry of PSC should be aimed at to achieve a more reliable prognosis of stratospheric ozone depletion.

### 4.3 Comparison of measurements with model calculations

The measured balloon-borne  $\text{ClO}$  profile (Figure 7, top left) shows a peak at about 450–550K (19–23km), indicating substantial chlorine activation from the  $\text{HCl}$  and  $\text{ClONO}_2$  reservoirs and thus the potential for chemical  $\text{O}_3$  depletion in this region. Indeed, the HALOE  $\text{HCl}$  profile

(Figure 7, top right, black triangles) shows much lower mixing ratios when compared to the initial profile ( $\star$ ). Further, an ozone loss of about 35% is derived at about 500K (Woyke et al., 1999) as the difference between the initial value ( $\star$ ) and the measured ozone profile (solid line in Figure 7, bottom left). As expected for a compound occurring in active form in the lower stratosphere without the need for heterogeneous activation, the observed BrO (Figure 7, lower right) shows very little variation with altitude.

With respect to ClO, the models can reproduce the shape of the measured profile, but with a scatter which is larger than the errors of the measurement, especially in the region of high ClO mixing ratio or strong ClO gradient. The three groups of models discussed in Section 4.2 are again found in this scatter: the models of group 1 (lowest chlorine activation, but most realistic assumptions for  $S_{\text{NAT}}$  and  $\gamma$ , e.g. turquoise and red) will produce the smallest amount and those of group 3 (strongest chlorine activation, e.g. green) the highest ClO. Altogether, a tendency to overestimate ClO is seen.

This tendency is also seen in the simulated BrO<sup>4</sup>. The scatter in BrO is due to both differences in reaction schemes and photolysis rates: the remaining inorganic bromine is mainly in the form of BrCl that is formed from a minor channel of the reaction BrO+ClO and is destroyed by BrCl photolysis. From a comparison of the BrO diurnal cycles of ARCTIC 1 (GPH, standard photolysis rates) with ARCTIC 1 (GPH, individual photolysis rates) it is deduced that the differences in BrO are caused by both the simulated ClO and mainly by the BrCl photolysis rates.

The scatter of model results around the HCl profile in this height region is much less pronounced.

From Figure 7 (bottom left) it also can be seen that the scatter of model results is small for O<sub>3</sub> and represents well the observed ozone loss up to the 475K level and again for 675K. However, none of the models can reproduce the measured stratospheric ozone loss in the height range of strongest ozone depletion (500 – 600K). Here, all the models underestimate the cumulative ozone loss by a factor of about two. The underestimated ozone loss is especially remarkable because most of the models clearly overestimate ClO and BrO, which should lead to a chemical ozone depletion stronger than that observed. Nevertheless, the three model groups can again be identified when taking into account that higher ClO leads to lower O<sub>3</sub>. It should be noted that those models closest to the observed ozone loss belong to model group 3 with the simplest assumptions for heterogeneous chemistry settings and the strongest overestimation of ClO.

The hypothesis that the ozone loss is underestimated by the models by about a factor of two is strengthened when bearing in mind that, on the one hand, the measured ozone loss in this

---

<sup>4</sup>the model MPIC (pink) is not represented in this figure because its bromine chemistry is not complete.

altitude range is confirmed by other methods (Woyke et al., 1999 and Section 4.1) and, on the other hand, the model results already represent their largest possible scatter and will not reach the observed values even if crucial model input parameters are changed within reasonable limits (Section 4.1). Further, this discrepancy is also found by other studies (for example the Match studies by Becker et al., 1998, Becker et al. 2000a, Rex et al. 2000, and the study by Goutail et al. 1999). In summary, this supports the conclusion that stratospheric ozone chemistry may not yet be completely understood.

## 5 Summary

Within the framework of a stratospheric chemistry model intercomparison various box, 2-D and 3-D models are compared for a broad band of chemical situations in the polar winter stratosphere. The focus of the study was to extensively compare the chemistry modules of the participating models for these conditions.

As the models aim to represent the current understanding of stratospheric chemistry they are expected to agree with each other under the controlled conditions of prescribed photolysis frequencies and PSC microphysics. Therefore, several prescribed Arctic and Antarctic scenarios were compiled for the year 1995 and two types of model runs were then performed: in the first runs only gas phase chemistry was considered while both gas phase and heterogeneous chemistry was enabled in the second version.

The mean ozone loss, chosen here as a measure of the agreement of the models, covers the wide range from about 4% to 80% depending on the specific scenario. Peak simulated ozone loss rates are 40 – 60 ppbv/day for the Arctic and  $\approx 130$  ppbv/day for the Antarctic scenarios.

The scatter of all model simulations around the mean percentage total ozone loss amounts to only 0.2 – 3.3% (absolute units) for the prescribed scenarios. Likewise, in these scenarios the species  $\text{HNO}_3$ ,  $\text{ClONO}_2$ ,  $\text{HCl}$ ,  $\text{ClO}$  and  $\text{Cl}_2\text{O}_2$  as well as the reaction surfaces  $S_{\text{STS}}$ ,  $S_{\text{NAT}}$  show good agreement. The agreement between the models is better for the pure gas phase indicating a sensitivity to details of the formulation of the heterogeneous chemistry modules.

Two additional results were derived from the prescribed scenarios without heterogeneous chemistry: the use of different photolysis modules and the assumptions concerning  $\text{HCl}$  source reactions implemented in the models do not influence the ozone loss to any great extent.

To investigate the actual differences between the models, an unprescribed Arctic case study was performed, where the individual schemes for both the photolysis and PSC microphysics are applied in the models. The scatter of model simulations around the mean percentage total

ozone loss increases to 6.7% (absolute units) in this scenario, caused by differences in the conversion processes of the chlorine reservoirs  $\text{ClONO}_2$  and  $\text{HCl}$  to the active chlorine compounds  $\text{ClO}$  and  $\text{Cl}_2\text{O}_2$ . Two settings of the microphysics and chemistry of polar stratospheric clouds (PSC) are identified as sources of the larger scatter of the model simulations: the supersaturation required for NAT formation,  $S_{\text{NAT}}$ , and the temperature dependence of the heterogeneous reaction probabilities,  $\gamma(1/T)$ . Those models using the most realistic assumptions about these parameters consequently simulate the most representative ozone chemistry.

The unprescribed Arctic case study also provides the opportunity to verify the model calculations by means of measurements in the Arctic vortex. As a result of this comparison it is found that the ozone loss is underestimated by all models by a factor of about two at the altitude of strongest ozone loss. This study indicates –in the same way as earlier work (Becker et al., 1998; Goutail et al. 1999, Becker et al. 2000a; Rex et al. 2000)– that the current knowledge of the stratospheric ozone chemistry may be incomplete.

The input data employed in the intercomparison and the corresponding model results are available (see Appendix) and may be used as a benchmark, e.g. to test newly developed models.

## Acknowledgments

The work was funded by the BMBF under contract 01L09525/0. The authors would like to thank Dr. Martin Dameris as one of the initiators and supporters of the project to compare the german stratospheric chemistry models. They also greatly acknowledge Mrs. Carter–Sigglow from the Language Service of the Research Center Jülich for improving the english language of the manuscript.

## Appendix

All the material necessary to repeat the runs of the model intercomparison can be found at:

[http://www.fz-juelich.de/icg/icg1/www\\_export/user/model\\_compare/model\\_compare.html](http://www.fz-juelich.de/icg/icg1/www_export/user/model_compare/model_compare.html)

In addition, initialization and results for all investigated chemical species of the scenarios not shown here (prescribed scenarios at the 420K and 600K levels as well as at all levels of the unprescribed ARCTIC CASE STUDY) are shown at this web site. We invite other groups to join the intercomparison and would be interested to hear about the results.



## References

- Becker, G., R. Müller, D. S. McKenna, M. Rex and K. S. Carslaw (1998): Ozone loss rates in the Arctic stratosphere in the winter 1991/92: Model calculations compared with Match results, *Geophys. Res. Lett.*, **25**, 4325–4328.
- Becker, G., R. Müller, D. S. McKenna, M. Rex, K. S. Carslaw and H. Oelhaf (2000a): Ozone loss rates in the Arctic stratosphere in the winter 1994/1995: Model simulations underestimate results of the Match analysis, *J. Geophys. Res.*, **105**, 15175–15184.
- Becker, G., J. U. GroöB, D.S. McKenna and R. Müller (2000b): Stratospheric photolysis frequencies: Impact of an improved numerical solution on the radiative transfer equation, *J. Atmos. Chem.*, **37**, 217–229.
- Blindauer, C., V. Rozanov and J.P. Burrows (1996): Actinic flux and photolysis frequency comparison computations using the Model PHOTOGT. *J. Atmos. Chem.*, **24**, 1–24.
- Brasseur, G., M. H. Hitchman, S. Walters, M. Dymek, E. Falise, and M. Pirre (1990): An interactive chemical dynamical radiative two-dimensional model of the middle atmosphere, *J. Geophys. Res.*, **95**, 5639–5655.
- Brasseur, G.P., X.X. Tie, P.J. Rasch, F. Lefèvre (1997): A three-dimensional simulation of the Antarctic ozone hole: Impact of anthropogenic chlorine on the lower stratosphere and upper troposphere. *J. Geophys. Res.*, **102**, 8909–8930.
- Brühl, C. and P.J. Crutzen (1989): On the disproportionate role of tropospheric ozone as a filter against solar UV-B radiation. *Geophys. Res. Lett.*, **16**, 703–706.
- Carslaw, K., B. Luo and T. Peter (1995): An analytic expression for the composition of aqueous  $\text{HNO}_3\text{-H}_2\text{SO}_4$  stratospheric aerosols including gas phase removal of  $\text{HNO}_3$ , *Geophys. Res. Lett.*, **22**, 1877–1880.
- Carslaw, K., T. Peter and S.L. Clegg (1997): Modeling the composition of liquid stratospheric aerosols. *Rev. Geophys.*, **35**(2), 125–153.
- Carver, G., P. Brown and O. Wild (1997): The ASAD atmospheric chemistry integration package and chemical reaction data base. *Comp. Phys. Comm.*, **105**, 197–215.
- Crutzen, P.J. and U. Schmailzl (1983): Chemical budgets of the stratosphere, *Planet. Space Sci.*, **31**, 1009–1032.

- DeMore, W.B., S.P. Sander, D.M. Golden, R.F. Hampson, M.J. Kurylo, C.J. Howard, A.R. Ravishankara, C.E. Kolb and M.J. Molina (1997): Chemical kinetics and photochemical data for use in stratospheric modeling, *JPL Publication 97-4, Jet Propulsion Laboratory, Pasadena*.
- Finkbeiner, M., J.N. Crowley, O. Horie, R. Müller, G.K. Moortgat and P.J. Crutzen (1995): The reaction between HO<sub>2</sub> and ClO: Product formation between 210 K and 300 K. *J. Phys. Chem.*, **99**, 16264–16275.
- Gidel, L.T., P.J. Crutzen and J. Fishman (1983): A two-dimensional photochemical model of the atmosphere; 1: Chlorocarbon emissions and their effect on stratospheric ozone. *J. Geophys. Res.*, **88**, 6622–6640.
- Goutail F., et al. (1998): Total ozone depletion in the Arctic during the winters of 1993-94 and 1994-95. *J. Atmos. Chem.*, **32**, 35-59.
- Goutail, F., et al. (1999): Total ozone depletion in the Arctic during the winters of 1993-94 and 1994-95. *J. Atmos. Chem.*, **32**, 35–59.
- Granier, C., and G. Brasseur (1992): Impact of heterogeneous chemistry on model predictions of ozone changes, *J. Geophys. Res.*, **97**, 18015-18033.
- Groß, J.-U. (1996): Modelling of Stratospheric Chemistry based on HALOE/UARS Satellite Data. *PhD thesis University of Mainz*.
- Günther, G., B.C. Krüger and A. Ebel (1995): Chemistry and transport at the vortex edge in the presence of breaking planetary waves. *Polar Stratospheric Ozone, Pub.: European Commission, Air Pollution Report 56*, 32–37.
- Hansen, G., T. Svenøe, M. P. Chipperfield, A. Dahlback and U.-P. Hoppe (1997): Evidence of substantial ozone depletion in winter 1995/96 over Northern Norway. *Geophys. Res. Lett.*, **24**, 799–802.
- Hanson, D.R. and K. Mauersberger (1988): Laboratory studies of the nitric acid trihydrate: Implications for the south polar stratosphere. *Geophys. Res. Lett.*, **15**, 855-858.
- Hendricks, J., E. Lippert, H. Petry and A. Ebel (1999): Heterogeneous reactions on and in sulfate aerosols: implications for the chemistry of the midlatitude tropopause region. *J. Geophys. Res.*, **104**, 5531–5550.

- Kröger, B.C. and P. Fabian (1986): Model calculations about the reduction of atmospheric ozone by different halogenated hydrocarbons. *Ber. Bunsenges. Phys. Chem.*, **90**, 1062–1066.
- Lary D.J. and J.A. Pyle (1991): Diffuse Radiation, Twilight, and Photochemistry - I *J. Atmos. Chem.*, **13**, 373-406.
- Lipson, J. B., M.J. Elrond and T.W. Beiderhase and L.T. Molina and M.J. Molina (1997): Temperature dependence of the rate constant and branching ratio for the OH + ClO reaction *J. Chem. Soc., Faraday Trans.*, **93**, 2665-2673.
- Madronich S. (1987): The Atmosphere and UV-B Radiation at Ground Level *Environmental UV Photobiology*, New York.
- Müller, R., P. J. Crutzen, J.-U. Groö, C. Brühl, J. M. Russel III, and A. F. Tuck (1996): Chlorine activation and ozone depletion in the Arctic vortex: Observations by the Halogen Occultation Experiment on the Upper Atmosphere Research Satellite. *J. Geophys. Res.*, **101**, 12531–12554.
- Park, J. H., M. K. W. Ko, C. H. Jackman, R. A. Plumb, J. A. Kaye and K. A. Sage (1999): Models and Measurements Intercomparison II. *NASA report, NASA/TM-1999-209554*.
- Pierson, J. M., K. A. McKinney, D. W. Toohey, J. Margitan, U. Schmidt, A. Engel and P. A. Newman (1999): An investigation of ClO photochemistry in the chemically perturbed Arctic vortex. *J. Atmos. Chem.*, **32**, 61-81.
- Rex, M., et al. (1998): In situ measurements of stratospheric ozone depletion rates in the Arctic winter 1991/92: A Lagrangian approach. *J. Geophys. Res.*, **103**, 5843–5853.
- Rex, M., R. Lehmann, R. J. Salawitch, M. L. Santee and J. W. Waters (2000): Theory and observation of Arctic ozone loss rates. *Proceedings of the Quadrennial Ozone Symposium, Sapporo, Japan*, 249-250.
- Röth, E.-P., 1992, A Fast Algorithm to Calculate the Photonflux in Optically Dense Media for Use in Photochemical Models, *Ber. Bunsenges. Phys. Chem.*, **96**, 417-420.
- Ruhnke, R., W. Kouker, and T. Reddmann (1999): The influence of the OH + NO<sub>2</sub> + M reaction on the NO<sub>y</sub> partitioning in the Arctic winter 1992/93 as studied with KASIMA *J. Geophys. Res.*, **104**, 3755-3772.

Woyke, T., R. Müller, F. Stroh, D.S. McKenna, A. Engel, J.J. Margitan, M. Rex, K.S. Carslaw (1999): A test of our understanding of ozone chemistry in the Arctic polar vortex using in-situ measurements of ClO, BrO, and O<sub>3</sub> in the 1994/95 winter, *J. Geophys. Res.*, **104**, 18,755–18,768.

Zdunkowski, W. G. (1980): An investigation of the structure of typical two-stream methods for the calculation of solar fluxes and heating rates in clouds. *Beitr. Phys. Atm.*, **53**, 147-166.